



저작자표시-비영리-변경금지 2.0 대한민국

이용자는 아래의 조건을 따르는 경우에 한하여 자유롭게

- 이 저작물을 복제, 배포, 전송, 전시, 공연 및 방송할 수 있습니다.

다음과 같은 조건을 따라야 합니다:



저작자표시. 귀하는 원저작자를 표시하여야 합니다.



비영리. 귀하는 이 저작물을 영리 목적으로 이용할 수 없습니다.



변경금지. 귀하는 이 저작물을 개작, 변형 또는 가공할 수 없습니다.

- 귀하는, 이 저작물의 재이용이나 배포의 경우, 이 저작물에 적용된 이용허락조건을 명확하게 나타내어야 합니다.
- 저작권자로부터 별도의 허가를 받으면 이러한 조건들은 적용되지 않습니다.

저작권법에 따른 이용자의 권리는 위의 내용에 의하여 영향을 받지 않습니다.

이것은 [이용허락규약\(Legal Code\)](#)을 이해하기 쉽게 요약한 것입니다.

[Disclaimer](#)

**A green process of polyampholyte-grafted single walled carbon
nanotubes for enhanced anticancer drug delivery**

Advisor: Prof. Kwon Taek Lim

By

Phan Quoc Thang

A thesis submitted in partial fulfillment of the requirements for the degree of
Master of Science

in Department of Display Engineering, The Graduate School,

Pukyong National University

February 2020

**A green process of polyampholyte-grafted single walled carbon
nanotubes for enhanced anticancer drug delivery**

A dissertation

By

Phan Quoc Thang

Approved by:



Dedicated to My Loving Parents...

Phan Van Dong

Lai Thi Tuyet Nhung

And

My "Little" Piffy



ABSTRACT

Polyampholytes are polymers including modified groups that can exhibit both a negative and a positive charge is wide attention for application in multidisciplinary fields such as biochemistry, biomaterials and pharmaceutical. In this dissertation, we report a novel process for surface modified single-walled carbon nanotubes (SWCNTs) as drug nanocarriers by using facile and green synthetic methods. Firstly, polyampholytic alternating polymers having furfuryl amine and 3-(dimethylamino)-1-propylamine as functional groups were prepared via one-pot thiol-ene chemistry in sustainable conditions. The monomer was prepared by the conjugation between maleic anhydride and thiolactone. Then, the polyampholytes were synthesized by one-pot two-step reaction through the amine-thiol-ene “click” chemistry. The alternating polymers were characterized by proton nuclear magnetic resonance (^1H NMR) and Fourier-transform infrared spectroscopy (FTIR). The anti-fouling of polyampholytes were performed and investigated by Ultraviolet–visible spectroscopy (UV-Vis).

Furthermore, the obtained polymers were then used to a direct functionalization onto the surface of SWCNTs through Diels-Alder click reaction conducted in aqueous media under ultrasonication. The resulting hybrid was characterized by FT-IR, Thermogravimetric analysis (TGA), Raman spectroscopy and UV-vis measurements. The hybrid improved the drug loading content up to 150 wt.%, indicating that they are potential doxorubicin (DOX) delivery nano-vehicles. Moreover, the in-vitro drug release profiles showed that there was a burst release of DOX at pH 5.5 under an acidic condition in microenvironment of tumor cells, in contrast with a lower release rate at pH 7.4 in the physiological condition. Significantly, we believe that the new facile grafting process approach can be reduced the using of organic solvent in preparation of drug nanocarriers.

요약

Polyampholytes 는 음전하와 양전하를 모두 나타낼 수 있는 개질된 그룹을 포함하는 중합체이며 생화학, 생체 재료 및 제약과 같은 다양한 분야에 적용하기 위해 주목되고 있다. 중합체 구조 및 특성은 인접하게 하전 된 Polyampholytes 그룹의 분자 내 이온 결합으로 제어될 수 있다. 이 연구는 손쉬운 녹색 합성 방법을 사용하여 약물 전달체로 표면이 개질된 single-walled carbon nano tubes(SWCNT)에 대한 새로운 방법을 제시한다. 먼저 작용기로서 furfuryl amine 과 3-(dimethylamino)-1-propylamine 를 갖는 polyampholytic alternating 고분자는 one-pot thiol-ene 방법으로 지속 가능한 조건에서 제조하였다. 얻어진 고분자는 Diels-Alder click 반응을 통해 SWCNT 의 표면에 적용하였다. 이것은 약물 전달 함량을 최대 150%까지 개선시켰고 이것은 잠재적인 doxorubicin (DOX) delivery nano 운반체임을 나타낸다. 또한 생리학적 조건에서 pH 7.4 기준의 낮은 방출 속도와는 대조적으로 종양 세포의 미세 환경 속에서는 pH 5.5 에서 폭발적인 DOX 의 방출을 나타냈다. 결과적으로 이러한 쉬운 grafting 공정 접근은 약물 나노 전달체에서 유기용매의 사용을 줄일 수 있다.

TABLE OF CONTENTS

CHAPTER 1: GENERAL INTRODUCTION	1
1.1. Introduction to drug delivery carriers	1
1.2. Application of functional polymers in nanocarrier formulation	2
1.3. Introduction to polyampholytes	4
1.4. Thiol-ene step-growth addition polymerization in the preparation of polyampholytes	5
1.5. Diels-Alder “click” reaction	7
1.6. Introduction to carbon nanotubes and its biomedical application	8
1.7. Aim and outline of this thesis	9
1.8. References.....	10
CHAPTER 2: SYNTHESIS, PROPERTIES AND CHARACTERIZATIONS OF FUNCTIONAL POLYAMPHOLYTES	15
2.1 Introduction.....	15
2.2 Experimental section.....	17
2.2.1 Materials	17
2.2.2 General procedure for synthesis of conjugated monomer	17

2.2.3 Polymerization of polyampholytes via thiol-ene chemistry	18
2.2.4 Protein adsorption assay	18
2.2.5 Characterization	18
2.3 Results and discussion	19
2.3.1 Synthesis and characterization of functional polyampholytes.....	19
2.3.2 The isoelectric points and anti-fouling property of polyampholytes.....	22
2.4 Conclusions	24
2.5 References	24
CHAPTER 3: POLYAMPHOLYTES GRAFTED ONTO SINGLE-WALLED CARBON NANOTUBES BY DIELS-ALDER REACTION AND ITS APPLICATION IN DRUG DELIVERY	26
3.1 Introduction.....	26
3.2 Experimental section.....	27
3.2.1 Materials	27
3.2.2 Synthesis of SWCNTs/PMTs hybrids	28
3.2.3 Characterization.....	28
3.2.4 In-vitro drug loading and release study	28
3.2.5 Cell viability	29

3.3 Results and discussion30

 3.3.1 Surface functionalization of SWCNT.....30

 3.3.2 In-vitro drug loading and release study34

 3.3.3 Cytotoxicity of blank PMT1/SWCNTs and DOX/PMT1/SWCNTs.....37

3.4 Conclusions.....38

3.5 References.....39



LIST OF FIGURES

Figure 1-1. Different types of nanocarriers have used for drug delivery.....	2
Figure 1-2. Some of the functional groups exhibiting stimuli-responsive characteristic.	3
Figure 1-3. a) Polyampholyte bearing both negative and positive charges statistically distributed along the polymer backbone, and b) polyzwitterion, bearing both charges in every repeating unit.	5
Figure 1-4. Step-growth polymerization mechanisms of (a) thiol-ene and (b) thiol-yne photopolymerization reactions.....	6
Figure 1-5. Classification of carbon nanotubes.	9
Figure 2-1. The ¹ H NMR spectrum of Ma-T1a in DMSO- <i>d</i> ₆	20
Figure 2-2. ¹ H NMR spectra of PMT in D ₂ O.....	20
Figure 2-3. FT-IR spectra (a) Ma-T1a monomer, (b) PMT3, (c) PMT2 and (d) PMT 1.....	21
Figure 2-4. Protein adsorption study with BSA (standard) on the polyampholytic polymers: PMT1, PMT2, PMT3 and Ma-T1a monomer; a) UV-vis absorption study and b) graphical representation of comparative protein adsorption.....	22
Figure 2-5. Potentiometric titration curve and first differential of polyampholytes: a) PMT1, b) PMT2 and c) PMT3.	23
Figure 3-1. FT-IR spectra PMT3 and SWCNTs before and after grafting with PMT3.....	31

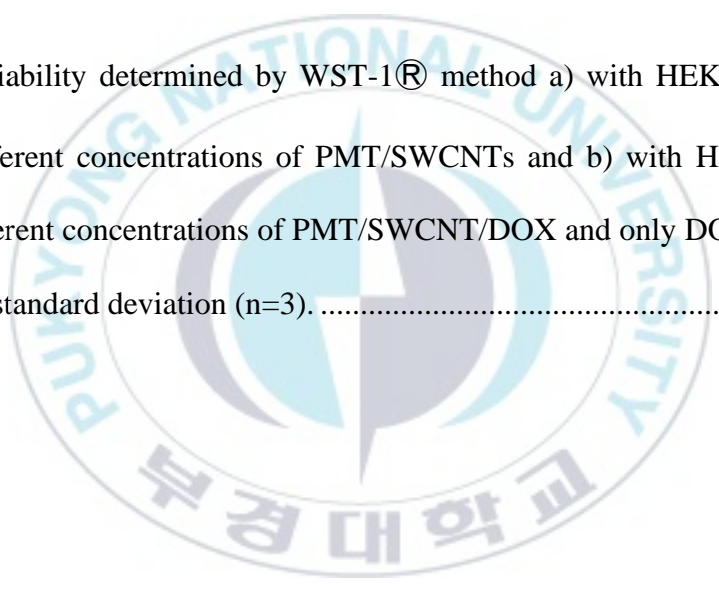
Figure 3-2. Raman spectra of SWCNTs (a) before modification, modified with (b) PMT1, (c) PMT2 and (d) PMT3.....32

Figure 3-3. a) TGA curves of pristine SWCNT, PMTs, and PMTs/SWCNT; b) UV-Vis spectra of aqueous dispersants of PMTs/SWCNT.33

Figure 3-4. TEM images of PMT/SWCNTs after the surface modification by DA reaction.34

Figure 3-5. pH responsive DOX release profile of DOX/PMT1/SWCNTs and DOX/PMT2/SWCNTs.....36

Figure 3-6. Cells viability determined by WST-1® method a) with HEK293 cells after 24 h incubation with different concentrations of PMT/SWCNTs and b) with HeLa cells after 24 h incubation with different concentrations of PMT/SWCNT/DOX and only DOX. Error bars above the bars indicates \pm standard deviation (n=3).38



LIST OF SCHEMES AND TABLES

Table 1-1. Some common Diels–Alder reactions in polymer synthesis and material science.....	7
Scheme 2-1. Preparation of functional polyampholytes for SWCNT grafting.	17
Table 2-1. Characteristics of resulting polymers with different ratios of functional groups.	19
Scheme 3-1. The preparation of polyampholytes grafted SWCNT for DOX loading.	27
Table 3-1. DOX encapsulation of PMT/SWCNTs.....	34



CHAPTER 1:

GENERAL INTRODUCTION

1.1. Introduction to drug delivery carriers

Although the standard chemotherapy has been successfully applied for clinical treatment, the main limitations of chemotherapy are the low bioavailability, the requirement of high-dose, undesirable side effects, multiple drug resistance of human body, and low accuracy targeting [1-5]. The main goal in the development of drug delivery carriers is to successfully control these release-related problems and deliver drugs to the specific sites of cancer therapy while decreasing side effects [6-9]. In past few years, the several types of material such as polymeric, metallic, and carbon-based materials were used as delivery agents for chemotherapeutic delivery and their structural characteristics that improve the therapeutic efficacy of anti-cancer drugs and will investigate scientific approaches in the field of tumor-therapy (**Figure 1-1**) [10-15].

To solve the drawbacks of conventional chemotherapeutic agents, nanocarriers have proved the potential to overcome these challenges by improving treatment efficacy while preventing cytotoxicity to normal cells based on the features such as great efficiency accumulation in cancer cell via the enhanced permeability and retention (EPR) effect and improve cellular uptake [16-19]. Especially, the active targeting therapy can be approached by interaction between nanocarriers containing anticancer-drug and tissues that overcome antigens expression. In past decade, among many nanoscale drug vehicles, polymeric nanoparticles, liposomes, and micelles have shown their excellent potential on the clinical impacts [20-24]. Up to now, although nanosized-vehicles offer many advantages to targeting drug delivery, their lack of biocompatibility, low bioavailability,

short-time in the circulation, inhomogeneous distribution and human antibody development raise concerns over their stability, in addition to the long-term application.

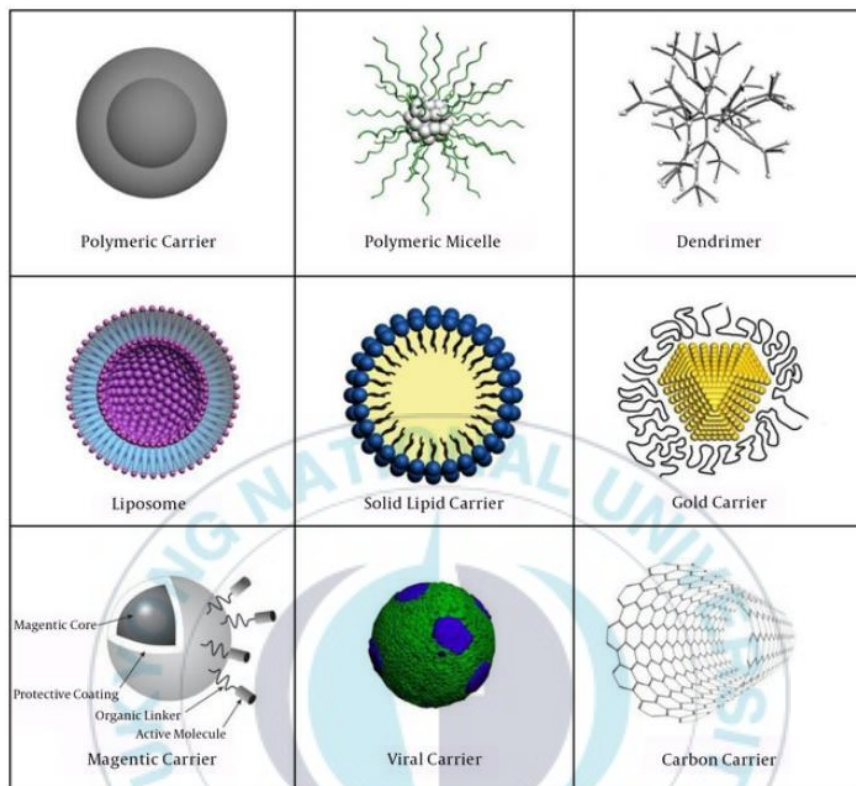


Figure 1-1. Different types of nanocarriers have used for drug delivery.

1.2. Application of functional polymers in nanocarrier formulation

Functional and smart polymers are currently applied in multidisciplinary engineering fields and especially it is playing a significant role in construction of targeted drug delivery systems due to their responsive characteristics towards intracellular stimuli. The formulation of delivery systems not only must be containing high biocompatibility and biodegradation properties but also having suitable mechanism for entrapping and releasing many kinds of active agents [25,26,27].

Polymers are becoming necessary in the formulation of drug delivery platform. Many researchers have investigated several kinds of functional polymers and applied in various stimuli such as thermal absorption, intensity of light, concentration of redox, pH environments, electric/magnetic fields [28,29,30]. Besides that, they have also combined multi-stimuli to improve and control effects on the physical/chemical properties of these polymers hence promote them smart, functional and highly suitable for numerous designs of drug delivery systems (**Figure 1-2**).

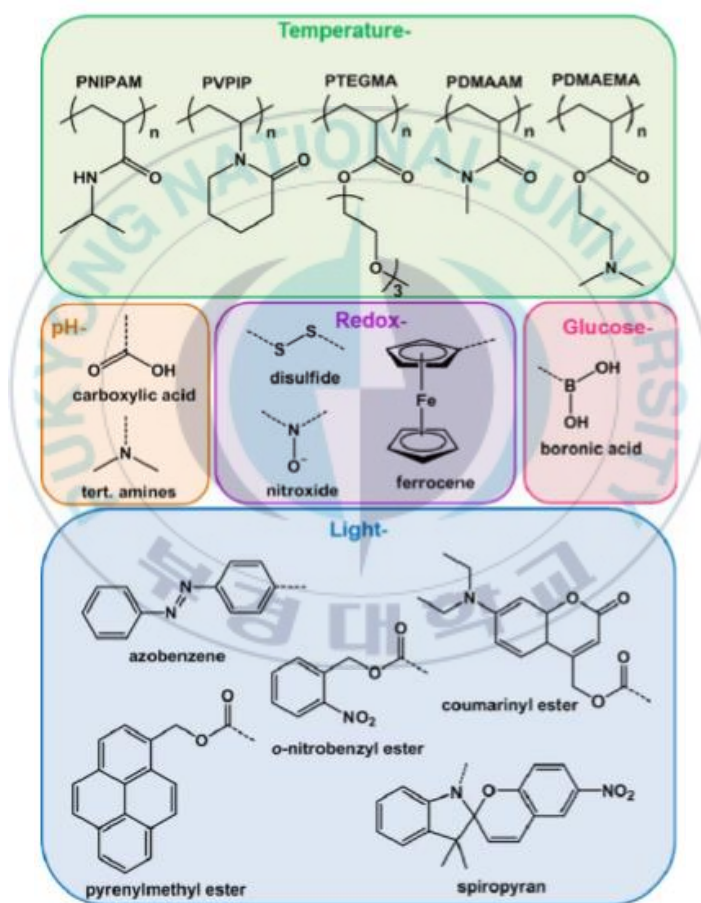


Figure 1-2. Some of the functional groups exhibiting stimuli-responsive characteristic.

Therefore, a significant number of publications have been focusing on polymers which could improve the delivery of drugs to appropriate sites such that the active agents are transported to the

target sites at the suitable time and dose. Polymeric-based nanocarriers are now proving potential for approaching the trend of drug delivery. There are many promising polymer technologies which might accelerate translation process of experiment-trial drug delivery systems towards clinical treatment. They can be acquired mostly due to the development of polymerization methods which are available, such as Atom transfer radical polymerization (ATRP) and Reversible addition–fragmentation chain-transfer polymerization (RAFT), which support for multi-diversity in terms of chemical conjugation, complex structure, narrow size and functionalization. In addition, these synthetic approaches including supramolecular assemblies and functionalized nanoparticles can be formulated which aim to the nanocarrier formulation [31,32].

1.3. Introduction to polyampholytes

Polyampholytes are polymeric varied charged systems composed of functional monomers. The strength of the charges as well as the polymer architecture influence both the mechanical properties and the response to external stimuli. The possibility of such dual control, and the unique traits of polyampholytes has led to their use for many and diverse purposes [33-37]. They are being considered for tissue engineering and pharmaceutical applications due to their unique characteristics including non-fouling properties, ability to deliver biomolecules to the body, and tunable mechanical properties. Polyampholyte materials are composed of mixtures of positively and negatively charged monomer subunits, resulting in an overall neutral charge. The non-fouling properties are likely derived from the formation of a strong hydration layer [36,37].

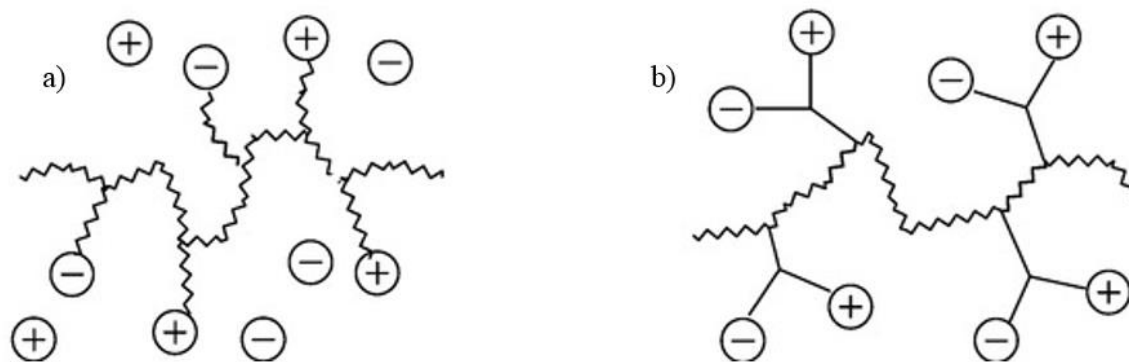


Figure 1-3. a) Polyampholyte bearing both negative and positive charges statistically distributed along the polymer backbone, and b) polyelectrolyte, bearing both charges in every repeating unit.

Recently, many current studies in polyampholyte indicated drug delivery takes advantage of the pH responsive behavior of polyampholyte systems. For example, chitosan based polyampholytes have recently been shown to have potential in protein delivery applications, as they have exhibited the ability to adsorb and desorb bovine serum albumin (BSA) in a pH dependent manner. However, a combination of design characteristics is required to optimize drug delivery that include biocompatibility, multifunctionality, and responsiveness to the microenvironment. The nanosized-gels have been evaluated for use as delivery systems and have shown tremendous promise due to the ability to control drug release, provide the drug protection from degradation, and target specific tissues. Some of the loading and controlled drug release techniques involve covalent bonding conjugation, passive/diffusion based, or through environmental stimuli, such as pH, reducing, and temperature [38,39,40].

1.4. Thiol-ene step-growth addition polymerization in the preparation of polyampholytes

Recently, precisely alternating functional polymers were prepared with thiolactone-containing monomers in one-pot procedure via amine-thiol-ene conjugation. Thiolactone chemistry has been

used as a facile platform for the synthesis of multifunctional polymers. Thiolactone rings were opened by aminolysis of several kinds of functional amines, and free thiols were released simultaneously and reacted with double bonds by nucleophilic Michael addition. When the thiol group and the double bond are present on the same molecule, this can result in step-growth thiol-ene polymerization [41,42].

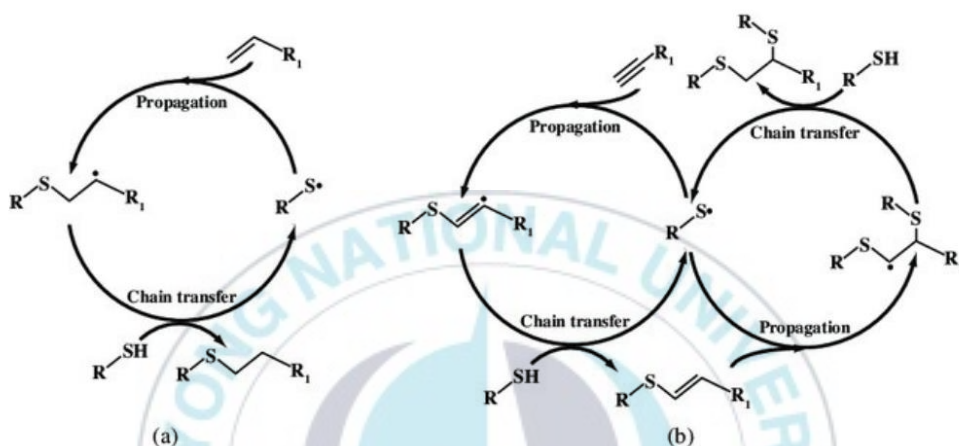


Figure 1-4. Step-growth polymerization mechanisms of (a) thiol-ene and (b) thiol-yne photopolymerization reactions.

In the present study, an innovative class of polyampholytes was synthesized via amine-thiol-ene conjugation, which contributes several advantages. Firstly, thiol-ene polymerization can be carried out in aqueous medium at room temperature and in the presence of oxygen. On the other hand, when compared with some kinds of radical polymerization of unsaturated monomers, there is no need for radical initiators or radical inhibitors for the polyampholyte precursors used in this method. Secondly, the distribution of the net charge along polymers can be controlled starting from the thiolactone-derived monomer and can be further varied by introducing multifunctional amine compounds. The distribution of the net charge along the polymer backbone has a significant effect on the physical and chemical properties. Finally, the solubility of polyampholytes can be improved

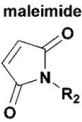
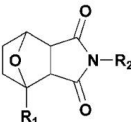
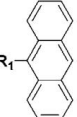
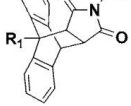
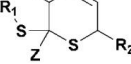
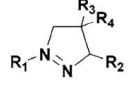
with additional polar or nonpolar functional groups that can be introduced via the aminolysis of thiolactone. Indeed, broad regions of insolubility of polyampholytes near the isoelectric point often limit their characterization and applications. Therefore, thiolactone chemistry contributes an important advancement in the field of polyampholytes and expands the range of functional and structural variations.

1.5. Diels-Alder “click” reaction

Over the last decade, the three main criteria of an ideal synthesis: efficiency, versatility, and selectivity are becoming the trend which requires the improvement in the use of rapid reactions. As a potential candidate, “click” reactions can be adapted to fulfill these criteria after several extensive reactions research. There are five main categories in this field: (i) Diels-Alder reaction, (ii) oxime/hydrazine formation (iii) azide-alkyne cycloaddition, (iv) thiol click reaction, and (v) 1,3-dipolar cycloaddition [43-46].

Diels–Alder (DA) reaction is one of the most common reactions used in organic chemistry and invented by Otto Diels and Kurt Alder who received the Nobel Prize in 1950 for their discovery. This reaction is classified as a [4+2] cycloaddition reaction which happens between an electron poor dienophile and a rich one to form an adduct with six stable members. Up to now, the DA reaction are increasing in the use synthetic organic chemistry and pharmaceutical as the most powerful technique. For instance, there were many complex architectures like graft, star, block, and cyclic polymer which were exploited by DA reaction. Moreover, it can be applied in the end-groups transformation, the surface modification of carbon nanotubes and design materials with self-healing ability [47].

Table 1-1: Some common Diels–Alder reactions in polymer synthesis and material science

Reagent A	Reagent B	Mechanism	Adduct	Conditions
 furan	 maleimide	[4 + 2] rDA cycloaddition reaction ^{5,20-23}		Between 25 and 120 °C without a catalyst reversible at temperatures higher than 120 °C
 anthracene	 maleimide	[4 + 2] DA cycloaddition reaction ^{24,25}		2 days under reflux in toluene without a catalyst
 dithioester	 diene	[4 + 2] HDA cycloaddition reaction ²⁶		10 min at r.t. catalyzed by trifluoroacetic acid
 tetrazine	 cyclooctene	[4 + 2] DA cycloaddition reaction inverse ²⁷⁻³⁰		40 min at 25 °C (100% yield) N ₂ is the only by-product

1.6. Introduction to carbon nanotubes and its biomedical application

Carbon nanotubes (CNT) are considered ideal materials for several applications, ranging from ultra-strong fibers to field emission displays. Recently, CNT have generated great interest in biology, where suitably modified CNT can serve as vaccine delivery systems or protein transporters [48,49,50].

CNT can be imaginatively produced by rolling up a single layer of graphene sheet (single-walled CNT; SWCNT), or by rolling up many layers to form concentric cylinders (multi-walled CNT; MWCNT). As-produced CNT, both SW and MW, are commercially available, with different structural details and variable degrees of purity [51,52]. Pristine CNT are completely insoluble in all solvents, which has generated some health concerns; consequently, their biological properties are being studied in terms of toxicity. The development of efficient methodologies for the chemical modification of CNT has stimulated the preparation of soluble CNT that can be employed in several biological applications, among which drug delivery appears to be particularly promising.

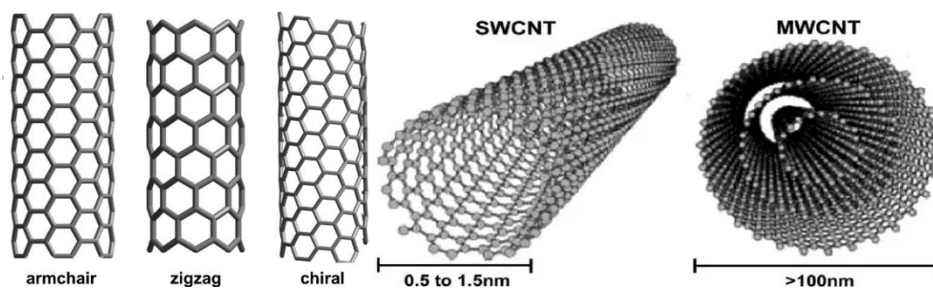


Figure 1-5. Classification of carbon nanotubes.

The search for new and effective drug delivery systems is a fundamental issue of continuous interest. A drug delivery system is generally designed to improve the pharmacological and therapeutic profile of a drug molecule. The ability of f-CNT to penetrate into the cells offers the potential of using f-CNT as vehicles for the delivery of small drug molecules. However, the use of f-CNT for the delivery of anticancer, antibacterial or antiviral agents has not yet been fully ascertained [53,54,55]. The development of delivery systems able to carry one or more therapeutic agents with recognition capacity, optical signals for imaging and/or specific targeting is of fundamental advantage, for example in the treatment of cancer and different types of infectious diseases. For this purpose, we have developed a new strategy for the multiple functionalization of CNT with different types of molecules.

1.7. Aim and outline of this thesis

The primary goal of this thesis is to apply new chemical techniques including thiol-ene chemistry and Diels-Alder reaction for the synthesis of stimuli-responsive drug delivery vehicles. The main study in this research is divided into two parts. In the first preparation, we focused on the synthesis of functionalized polyampholytes of D,L-homocysteine thiolactone hydrochloride and maleic anhydride by step-growth thiol-ene polymerization with furfuryl amine and 3-(dimethylamino)-1-propylamine were used as functional groups.

In the next part of this study, pH-responsive of polyampholyte grafted on the surface of single-walled carbon nanotubes (SWCNT) was synthesized by the Diels-Alder reaction. The morphology as well as in vitro drug release profile under physiology and acidic conditions were examined. Beside that, the cytotoxicity on the normal cell and against cancer cell were also investigated. We imply that the green and facile grafting process can be improved the preparation of nanocomposite and especially the applications of carbon nanotubes in drug delivery.

1.8. References

1. Gutteridge, W. E., *Br. Med. Bull.* **1985**, *41* (2), 162-168.
2. Marin, J. J.; Romero, M. R.; Blazquez, A. G.; Herraes, E.; Keck, E.; Briz, O., *Anti-Cancer Agents in Medicinal Chemistry (Formerly Current Medicinal Chemistry-Anti-Cancer Agents)* **2009**, *9* (2), 162-184.
3. Chidambaram, M.; Manavalan, R.; Kathiresan, K., *J. Pharm. Pharm. Sci.* **2011**, *14* (1), 67-77.
4. Lamm, D.; Van der Meijden, A.; Akaza, H.; Brendler, C.; Hedlund, P.; Mizutani, Y.; Ratliff, T.; Robinson, M.; Shinka, T., *Int. J. Urol.* **1995**, *2*, 23-35.
5. Cairo, M. S., **2000**.
6. Gelperina, S.; Kisich, K.; Iseman, M. D.; Heifets, L., *Am. J. Respir. Crit. Care Med.* **2005**, *172* (12), 1487-1490.
7. Allen, T. M.; Cullis, P. R., *Science* **2004**, *303* (5665), 1818-1822.
8. Kayser, O.; Lemke, A.; Hernandez-Trejo, N., *Curr. Pharm. Biotechnol.* **2005**, *6* (1), 3-5.
9. Saraf, S., *Fitoterapia* **2010**, *81* (7), 680-689.
10. Liu, Z.; Robinson, J. T.; Tabakman, S. M.; Yang, K.; Dai, H., *Mater. Today* **2011**, *14* (7-8), 316-323.

11. Carino, I. S.; Pasqua, L.; Testa, F.; Aiello, R.; Puoci, F.; Iemma, F.; Picci, N., *Drug Deliv.* **2007**, *14* (8), 491-495.
12. Kaufman, H. E., Drug delivery system. Google Patents: 1989.
13. Goldberg, M.; Langer, R.; Jia, X., *J. Biomater. Sci. Polym. Ed.* **2007**, *18* (3), 241-268.
14. Mitragotri, S.; Lahann, J., *Adv. Mater.* **2012**, *24* (28), 3717-3723.
15. Sastry, S. V.; Nyshadham, J. R.; Fix, J. A., *Pharm. Sci. Technolo. Today* **2000**, *3* (4), 138-145.
16. Middleton, M. R.; Margison, G. P., *The Lancet Oncology* **2003**, *4* (1), 37-44.
17. Duncan, R., *Anti-Cancer Drugs* **1992**, *3* (3), 175-210.
18. France, D. J.; Miles, P.; Cartwright, J.; Patel, N.; Ford, C.; Edens, C.; Whitlock, J. A., *The Joint Commission Journal on Quality and Safety* **2003**, *29* (4), 171-180.
19. Hurwitz, E., *Biopolymers: Original Research on Biomolecules* **1983**, *22* (1), 557-567.
20. Qiu, L. Y.; Bae, Y. H., *Pharm. Res.* **2006**, *23* (1), 1-30.
21. Napier, M. E.; DeSimone, J. M., *Journal of Macromolecular Science, Part C: Polymer Reviews* **2007**, *47* (3), 321-327.
22. Gillies, E. R.; Frechet, J. M., *Drug Discovery Today* **2005**, *10* (1), 35-43.
23. Jeong, B.; Choi, Y.; Bae, Y.; Zentner, G.; Kim, S., *J. Controlled Release* **1999**, *62* (1-2), 109-114.
24. Jabr-Milane, L.; van Vlerken, L.; Devalapally, H.; Shenoy, D.; Komareddy, S.; Bhavsar, M.; Amiji, M., *J. Controlled Release* **2008**, *130* (2), 121-128.
25. Nicolas, J.; Mura, S.; Brambilla, D.; Mackiewicz, N.; Couvreur, P., *Chem. Soc. Rev.* **2013**, *42* (3), 1147-1235.

26. Jabr-Milane, L. S.; van Vlerken, L. E.; Yadav, S.; Amiji, M. M., *Cancer Treat. Rev.* **2008**, *34* (7), 592-602.
27. Shao, P.; Wang, B.; Wang, Y.; Li, J.; Zhang, Y., *Journal of Nanomaterials* **2011**, *2011*, 17.
28. Zhu, Y.; Yang, B.; Chen, S.; Du, J., *Prog. Polym. Sci.* **2017**, *64*, 1-22.
29. Torchilin, V. P., *Adv. Drug Del. Rev.* **2006**, *58* (14), 1532-1555.
30. Singh, R.; Lillard Jr, J. W., *Exp. Mol. Pathol.* **2009**, *86* (3), 215-223.
31. Kumari, A.; Yadav, S. K.; Yadav, S. C., *Colloids Surf. B. Biointerfaces* **2010**, *75* (1), 1-18.
32. Kudaibergenov, S. E., *Polyampholytes: synthesis, characterization and application*. Springer Science & Business Media: 2012.
33. Katchalsky, A.; Miller, I. R., *J. Polym. Sci.* **1954**, *13* (68), 57-68.
34. Qingda, Z.; Zhuomei, L., *JOURNAL OF FUNCTIONAL POLYMERS* **1994**, *1*.
35. Dobrynin, A. V.; Colby, R. H.; Rubinstein, M., *J. Polym. Sci., Part B: Polym. Phys.* **2004**, *42* (19), 3513-3538.
36. Li, S.; Wu, Y.; Wang, J.; Zhang, Q.; Kou, Y.; Zhang, S., *J. Mater. Chem.* **2010**, *20* (21), 4379-4384.
37. Mironov, M. A.; Shulepov, I. D.; Ponomarev, V. S.; Bakulev, V. A., *Colloid. Polym. Sci.* **2013**, *291* (7), 1683-1691.
38. Kudaibergenov, S.; Koetz, J.; Nuraje, N., *Advanced Composites and Hybrid Materials* **2018**, *1* (4), 649-684.
39. Zurick, K. M.; Bernards, M., *J. Appl. Polym. Sci.* **2014**, *131* (6).
40. Asayama, S.; Nogawa, M.; Takei, Y.; Akaike, T.; Maruyama, A., *Bioconjugate Chem.* **1998**, *9* (4), 476-481.

41. Resetco, C.; Frank, D.; Kaya, N. U.; Badi, N.; Du Prez, F., *ACS Macro Letters* **2017**, 6 (3), 277-280.
42. Espeel, P.; Goethals, F.; Driessen, F.; Nguyen, L.-T. T.; Du Prez, F. E., *Polymer Chemistry* **2013**, 4 (8), 2449-2456.
43. Pasini, D., *Molecules* **2013**, 18 (8), 9512-9530.
44. Tiwari, V. K.; Mishra, B. B.; Mishra, K. B.; Mishra, N.; Singh, A. S.; Chen, X., *Chem. Rev.* **2016**, 116 (5), 3086-3240.
45. Karmakar, S.; Datta, A., *The Journal of Physical Chemistry B* **2015**, 119 (35), 11540-11547.
46. Gao, L.; Zhang, J.-h.; Chen, S.-h.; Zhang, D.-h., *Adhesion* **2013**, 34, 32-35.
47. Tasdelen, M. A., *Polymer Chemistry* **2011**, 2 (10), 2133-2145.
48. Bianco, A.; Kostarelos, K.; Prato, M., *Curr. Opin. Chem. Biol.* **2005**, 9 (6), 674-679.
49. He, H.; Pham-Huy, L. A.; Dramou, P.; Xiao, D.; Zuo, P.; Pham-Huy, C., *BioMed research international* **2013**, 2013.
50. Madani, S. Y.; Naderi, N.; Dissanayake, O.; Tan, A.; Seifalian, A. M., *International journal of nanomedicine* **2011**, 6, 2963.
51. Vardharajula, S.; Ali, S. Z.; Tiwari, P. M.; Eroğlu, E.; Vig, K.; Dennis, V. A.; Singh, S. R., *International journal of nanomedicine* **2012**, 7, 5361.
52. Zhang, Y.; Bai, Y.; Yan, B., *Drug Discovery Today* **2010**, 15 (11-12), 428-435.
53. Guldi, D. M.; Martín, N., *Carbon nanotubes and related structures: synthesis, characterization, functionalization, and applications*. John Wiley & Sons: 2010.
54. Eatemadi, A.; Daraee, H.; Karimkhanloo, H.; Kouhi, M.; Zarghami, N.; Akbarzadeh, A.; Abasi, M.; Hanifehpour, Y.; Joo, S. W., *Nanoscale research letters* **2014**, 9 (1), 393.

55. Madani, S. Y.; Tan, A.; Dwek, M.; Seifalian, A. M., *International journal of nanomedicine* **2012**, 7, 905.



CHAPTER 2:

SYNTHESIS, PROPERTIES AND CHARACTERIZATIONS OF FUNCTIONAL POLYAMPHOLYTES

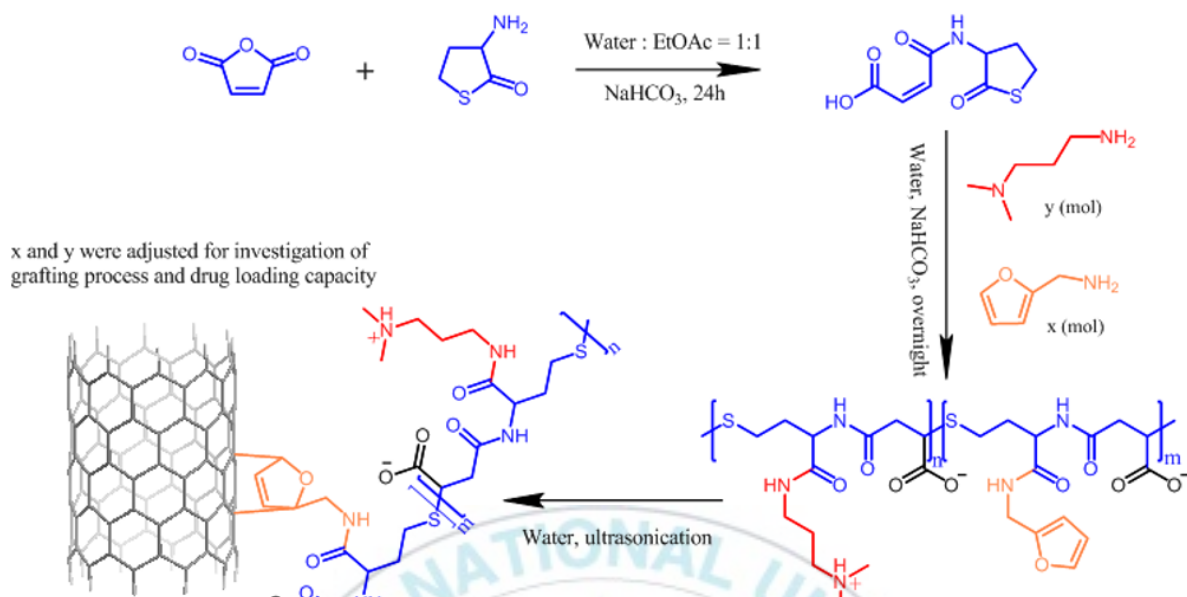
2.1 Introduction

In the drug administration, when nanocarriers enter a human body environment (extracellular fluid containing interstitial fluid and blood plasma), they are often adhered by proteins (protein corona). As a result, the properties of nanocarriers are affected by the protein corona, preventing the nanocarriers from cellular uptake significantly [1-4]. An interesting approach to avoid this effect is the zwitterionization of the surface of nanomaterials for acquiring anti-fouling properties. Polyampholyte polymers are a subclass of zwitterionic materials containing functional groups that can exhibit both negative and positive charges, which can be used as antifouling agents [5-8]. A strong hydration layer is formed through the electrostatic interaction, rendering efficient anti-fouling surfaces onto nanocarriers. In addition, they meet many requirements for an effective nanosized drug delivery vehicles such as prolongation of blood circulation time and “stealth ability” over several stages of immune system. Consequently, extremely weak interactions with serum proteins and high biocompatibility make them as valuable candidates for proteins destabilizing and drug delivery agents [9].

On the other hand, radical copolymerization is a common synthetic method for the preparation of polyampholytes with different unsaturated monomers. However, the adaption to various monomer compositions is assumed to be a limitation to the development of multiple functionalized polyampholytes. Thiolactone chemistry is a potential alternative process for the synthesis of

multifunctional polymers, such as alternating polymers, cyclic polymers, hyperbranched polymers, and polyelectrolytes [10-13]. Furthermore, this reaction can be performed in water at room temperature, which has significant advantages over other polymeric reactions using organic solvents. The functionalized polymers can be synthesized in one-pot two-step reaction through the amine-thiol-ene “click” chemistry, which is initiated from a double-bond conjugating in thiolactone. After that, the functionalized thiolactone moieties undergo the ring-opening reaction with several kinds of amines, releasing thiol groups. Furthermore, step-growth thiol-ene polymerization occurs readily between free thiols and the double bonds on the conjugated thiolactones, especially under basic conditions [14].

In this chapter, we demonstrated that firstly, the functional monomer based on maleic anhydride-thiolactone adduct (MA-TIa) was prepared by the addition reaction of D,L-homocysteine thiolactone hydrochloride and maleic anhydride. Then, the highly reactive thiolactone parts were reacted sequentially with different ratios of furfuryl amine and 3-(dimethylamino)-1-propylamine, resulting in polyampholytic alternating polymers (PMT) with furfuryl pendant moieties (**Scheme 2-1**).



Scheme 2-1. Preparation of functional polyampholytes for SWCNT grafting.

2.2 Experimental section

2.2.1 Materials

DL-Homocysteine thiolactone hydrochloride ($\geq 99.0\%$), maleic anhydride (99%), furfuryl amine (99%), 3-dimethylamino)-1-propylamine (99%), sodium bicarbonate ($\geq 99.7\%$), and dialysis bags were obtained from Sigma-Aldrich. Hydrochloric acid (HCl) (37%) was purchased from Duksan Pure Chemicals Co., Ltd (South Korea).

2.2.2 General procedure for synthesis of conjugated monomer

Ma-Tla was prepared by following the procedure in the previous report [14]. Briefly, 23 g (0.15 mol, 1.0 equiv.) of DL-homocysteine thiolactone hydrochloride was dissolved in 100 mL of water

and ethyl acetate (1:1) in a one-neck flask. At 0°C, 33.6 g (0.4 mol, 2.6 equiv.) of sodium carbonate was added into the solution, and then 19.7 g (0.2 mol, 1.3 equiv.) of maleic anhydride in acetone was added dropwise under vigorous stirring. The reaction solution was kept stirring for 3 h at room temperature. The white crystal was obtained after acidified by a 6 M hydrochloric acid solution. Next, the product (70 %) was filtered out, rinsed with 20 mL of water and dried in vacuo.

2.2.3 Polymerization of polyampholytes via thiol-ene chemistry

In a typical procedure, a solution of 1.72 g (8 mmol) of Ma-Tla dispersed in 12 mL water was placed at 0°C for 10 min before adding a solution of 1.008 g (12 mmol) of sodium bicarbonate in 20 mL water. The reaction mixture was kept stirring until it became a clear solution. Next, 12.8 mmol of a mixture of furfurylamine and 3-(dimethylamino)-1-propylamine was added into the solution. The reaction solution was kept stirring overnight at room temperature. The precipitated white polymer was collected from acetone and dried in vacuo.

2.2.4 Protein adsorption assay

The anti-fouling activity of the synthesized Ma-Tla monomer and PMTs were determined by the adsorption of a protein, bovine serum albumin (BSA) over polymer films. For the preparation of the polymer films, solutions of Ma-Tla monomer and PMTs (prepared in a 4:1 volume mixture of water and DMSO) were casted on glass slides dried at 50°C under vacuum condition. Afterwards, the slides were immersed separately into 10ml of BSA solution (2mg/ml, PBS 7.4) at 37°C for 24h. The data for BSA adsorption on Ma-Tla monomer and PMTs were collected by means of a UV-Visible spectrophotometer (at the wavelength of 286 nm).

2.2.5 Characterization

A JNM-ECP 600 MHz (JEOL, Japan) instrument was used to measure proton NMR spectra. An Agilent Cary spectrometer was operated in the range 4000-500 cm^{-1} with KBr pellets to investigate the Fourier transform infrared (FT-IR) spectra. Potentiometric titrations were performed on a NeoMet K2000 pH/Ion meter. The obtained polymer (100mg) was dissolved in 10 mL of 0.1 M NaOH (pH~12) and equilibrated by stirring for 1 h. Then, the samples were titrated with 1 M HCl in 50 μ L aliquots until pH~2.

2.3 Results and discussion

2.3.1 Synthesis and characterization of functional polyampholytes

The structure of Ma-Tla was confirmed by means of ^1H NMR spectroscopy, as shown in **Figure 2-1**. The peak which corresponds to the proton of secondary amines is observed at 9.26 ppm. Two protons on the double bond of alkylene groups are shown at 6.35 and 6.2 ppm. Since one of these protons is attached to the carbon directly linking to the carboxyl group, it shifts toward higher field. The proton peak of the isopropyl group is settled at 4.65 ppm due to the impact of the secondary amine group. In addition, methanediyl peaks next to the sulfur group are distributed at 3.4 and 3.25 ppm while the other methanediyl peaks appear at 2.35 and 2.1 ppm. The signal of the carboxyl group is hardly detected possibly due to the hydrogen bonding of –COOH with itself or the DMSO-*d*6 solvent.

Table 2-1. Characteristics of resulting polymers with different ratios of functional groups.

Polymer	Feed ratio (x:y)	Reaction ratio (n:m) ^a	pI ^b	Dissolved pH range ^b	Grafting density (%) ^c
PMT1	3 : 7	3.5 : 6.5	6.1	12-2	11.04

PMT2	5 : 5	5 : 5	4.7	12-2	11.93
PMT3	7 : 3	6 : 4	6.9	12-4	13.56

^a Calculated from integration of ¹H NMR signals in spectra acquired in D₂O, ^b Determined by potentiometric titrations curves, ^c Acquired from TGA analysis.

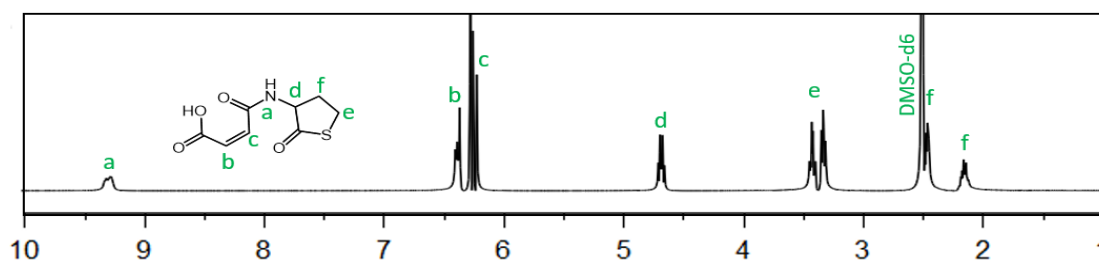


Figure 2-1. The ¹H NMR spectrum of Ma-TIa in DMSO-*d*₆.

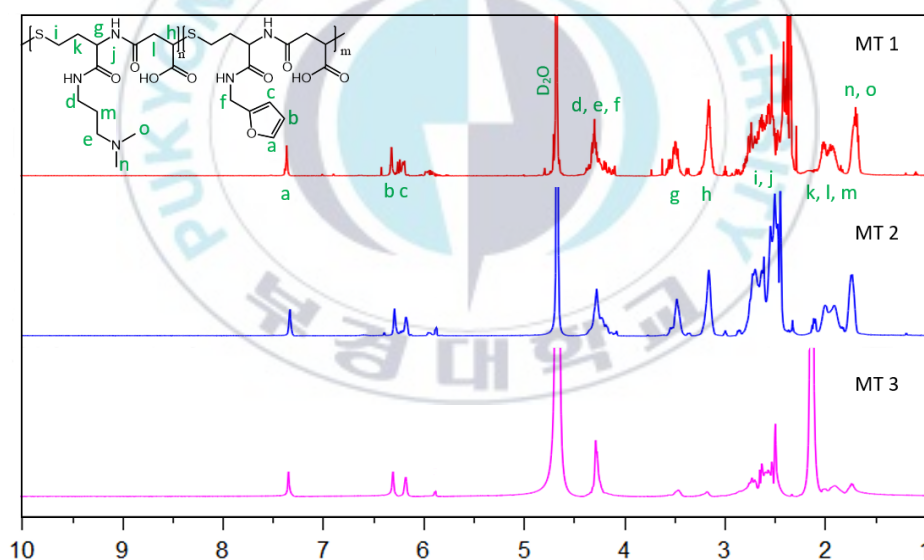


Figure 2-2. ¹H NMR spectra of PMT in D₂O.

Figure 2-2 depicts the ¹H NMR spectra of PMT. The signal of protons in furfuryl groups are shown at 7.35, 6.30, 6.2 and 4.27 ppm, whereas the peaks of the 3-(dimethyl amino)-1-propyl group were distributed in sequence at lower chemical shifts of 4.27, 2.05 – 1.80 and 1.76 – 1.63 ppm. All proton peaks of the polymer backbone are displayed in the range

of 3.55 to 2.45 ppm. The intensity of two peaks at 7.35 and 4.27 ppm were compared each other to determine the ratio of repeating units (n and m). As summarized in **Table 2-1**, the polymers with various repeating units whose ratios n:m were 6.08:3.91(for MT3); 5.31:4.69 (for MT2) and 3.44:6.56 (for MT1) could be prepared by adding various ratios of 3-(dimethylamino)-1-propylamine and furfurylamine into the one-pot reaction.

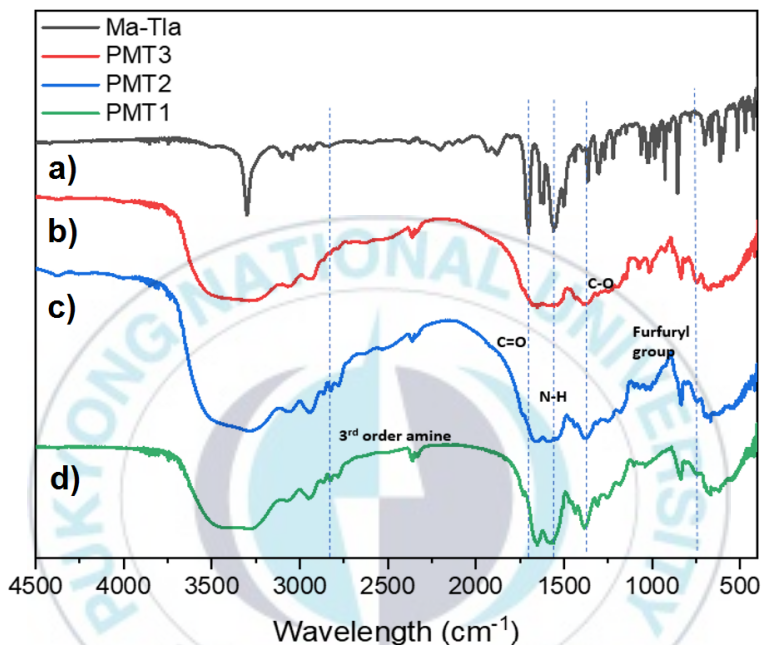


Figure 2-3. FT-IR spectra (a) Ma-TIa monomer, (b) PMT3, (c) PMT2 and (d) PMT 1.

PMTs were further characterized by means of FT-IR spectroscopy, as shown in **Figure 2-3**. Several characteristic peaks of PMTs emerged when compare with Ma-TIa monomers by modifying with furfuryl amine and 3-(dimethylamino)-1-propylamine. The FT-IR spectrum of PMTs displays characteristic bands of tertiary amine, secondary amine, carbonyl and furfuryl groups at 2650, 1603, 1700 and 1370 cm^{-1} , and at 600 and 750 cm^{-1} , respectively. In the spectrum of Ma-TIa (**Figure 2-3a**), the characteristic band of secondary amine groups at 1600 cm^{-1} is weaker than PMTs, verifying the successful transformation to the functional polymers through aminolysis.

Furthermore, the tertiary amine group (-N- stretch) and furfuryl group in **Figure 2-3a, b, and c** confirm the successful synthesis of PMTs with different ratios of two amines.

2.3.2 The isoelectric points and anti-fouling property of polyampholytes

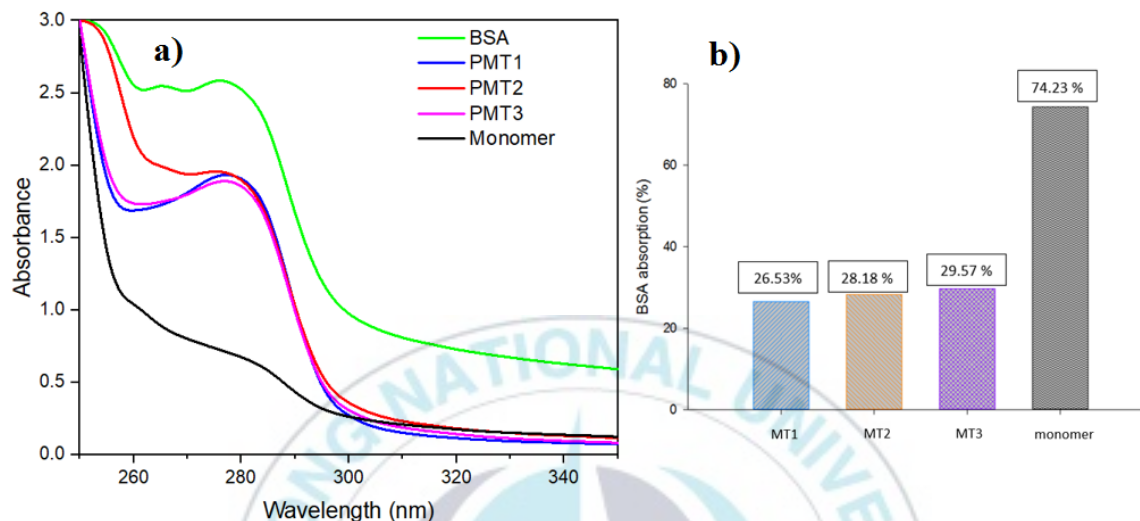


Figure 2-4. Protein adsorption study with BSA (standard) on the polyampholytic polymers: PMT1, PMT2, PMT3 and Ma-Tla monomer; a) UV-vis absorption study and b) graphical representation of comparative protein adsorption.

In order to investigate anti-fouling properties, we examined the BSA adsorption test for PMT1, PMT2, PMT3 and Ma-Tla monomers. As shown in **Figure 2-4**, the characteristic absorbance of BSA at 286 nm was reduced slightly for the three types of polyampholytic polymers (PMT1, PMT2, and PMT3) about 26.53 %, 28.18 % and 29.57%, respectively, compared with pure BSA (**Figure 2-4b**). It is suggested that the higher moieties of 3-(dimethylamino)-1-propylamine in the polymeric backbone reduced the protein adsorption probably owing to the increasing in anti-electrolyte effect by tunable net charge and charge density. In contrast, Ma-Tla showed much higher BSA adsorption (about 74.23 %) because

of non-charges in the structure. This result demonstrates that the polyampholytic PMTs contribute to the excellent anti-fouling properties.

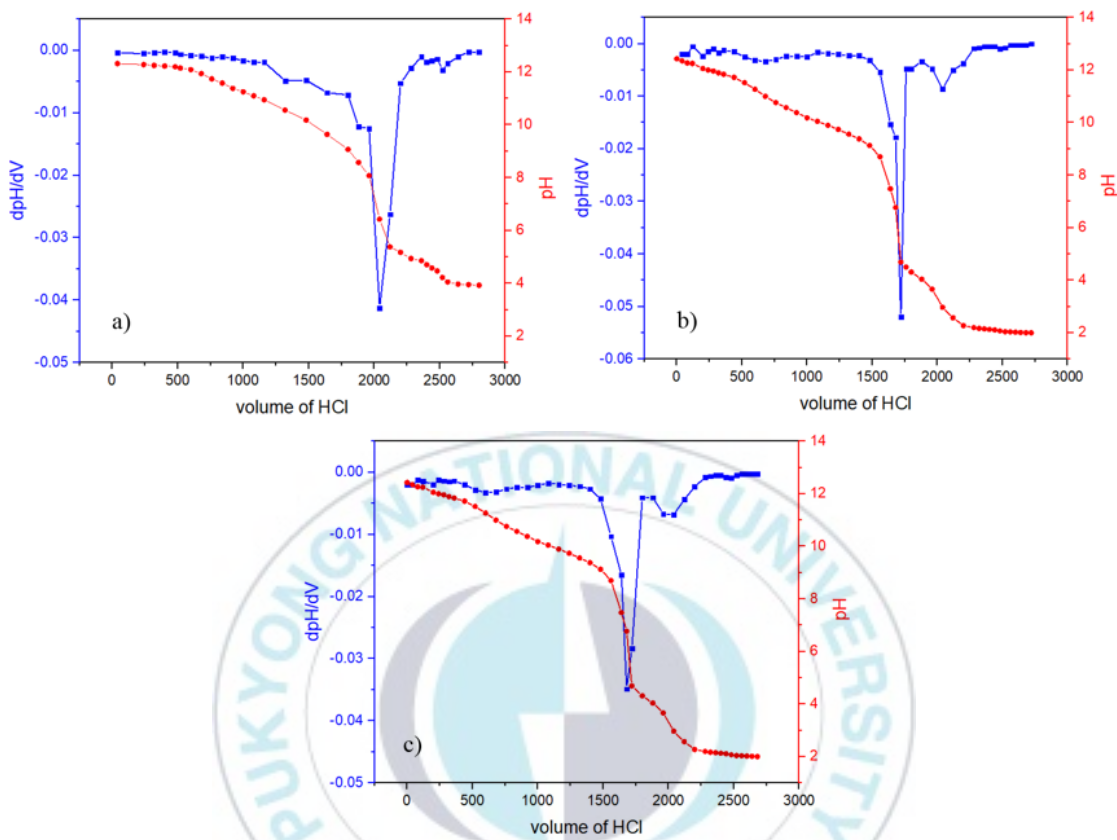


Figure 2-5. Potentiometric titration curve and first differential of polyampholytes: a) PMT1, b) PMT2 and c) PMT3.

The isoelectric points (pI) of the polyampholytes (PMT1, PMT2, and PMT3) were determined by potentiometric titration. The high solubility of alternating polyampholytes over a broad pH range is characteristic of the interactions between the adjacent ionic groups, which inhibit complete charge compensation within the polyampholyte that is typically associated with insolubility. As can be seen in Figure 2-5, the pI of PMT1 is 6.1 and pH range is 12-4, the pI of PMT2 is 4.7 and pH range is 12-2 and the pI of PMT3 is 6.9 and pH range is 12-2. These results indicate the high solubility of synthesized polyampholytes which can be applied to improve the hydrophilicity of grafted materials.

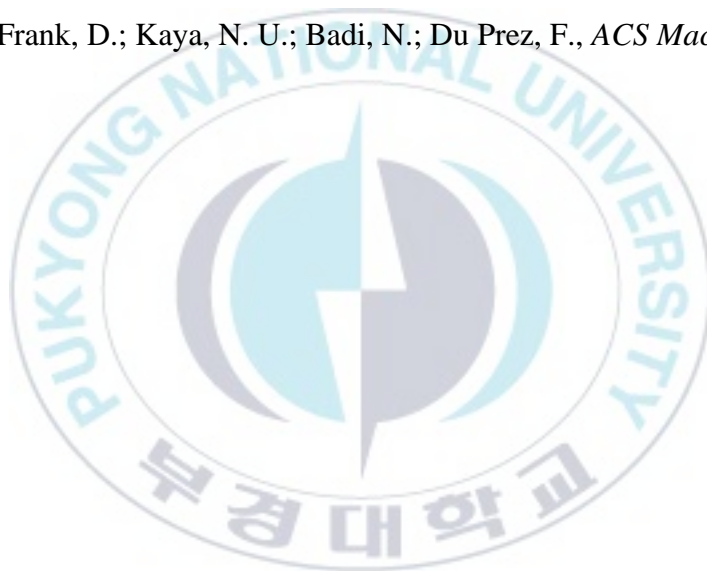
2.4 Conclusions

High stability and solubility polyampholytes were successfully synthesized by using thiol-ene chemistry with well-defined maleic anhydride-thiolactone adduct (MA-Tla), and its behaviors were systematically characterized by potentiometric titrations, protein adsorption assay, ¹H NMR and FTIR. These polyampholytes enhanced hydrophilic behavior in aqueous medium at room temperature at low and high pH, therefore, it can be used as coating materials for drug delivery applications.

2.5 References

1. Corbo, C.; Molinaro, R.; Parodi, A.; Toledano Furman, N. E.; Salvatore, F.; Tasciotti, E., *Nanomedicine* **2016**, *11* (1), 81-100.
2. Caracciolo, G., *Bioinspired, Biomimetic and Nanobiomaterials* **2013**, *2* (1), 54-57.
3. Schöttler, S.; Landfester, K.; Mailänder, V., *Angew. Chem. Int. Ed.* **2016**, *55* (31), 8806-8815.
4. Lee, Y. K.; Choi, E.-J.; Webster, T. J.; Kim, S.-H.; Khang, D., *International journal of nanomedicine* **2015**, *10*, 97.
5. Schroeder, M. E.; Zurick, K. M.; McGrath, D. E.; Bernards, M. T., *Biomacromolecules* **2013**, *14* (9), 3112-3122.
6. Zhao, T.; Chen, K.; Gu, H., *The Journal of Physical Chemistry B* **2013**, *117* (45), 14129-14135.
7. Zurick, K. M.; Bernards, M., *J. Appl. Polym. Sci.* **2014**, *131* (6).
8. Ayres, N.; Cyrus, C. D.; Brittain, W. J., *Langmuir* **2007**, *23* (7), 3744-3749.

9. Kisley, L.; Serrano, K. A.; Davis, C. M.; Guin, D.; Murphy, E. A.; Gruebele, M.; Leckband, D. E., *Biomacromolecules* **2018**, *19* (9), 3894-3901.
10. Li, G.; Xue, H.; Gao, C.; Zhang, F.; Jiang, S., *Macromolecules* **2009**, *43* (1), 14-16.
11. Denis, M. F. L.; Carballo, R. R.; Spiaggi, A. J.; Dabas, P. C.; Dall'Orto, V. C.; Martínez, J. M. L.; Buldain, G. Y., *React. Funct. Polym.* **2008**, *68* (1), 169-181.
12. Didukh, A. G.; Koizhaiganova, R. B.; Khamitzhanova, G.; Bimendina, L. A.; Kudaibergenov, S. E., *Polym. Int.* **2003**, *52* (6), 883-891.
13. Sanjuan, S.; Tran, Y., *Macromolecules* **2008**, *41* (22), 8721-8728.
14. Resetco, C.; Frank, D.; Kaya, N. U.; Badi, N.; Du Prez, F., *ACS Macro Letters* **2017**, *6* (3), 277-280.



CHAPTER 3:

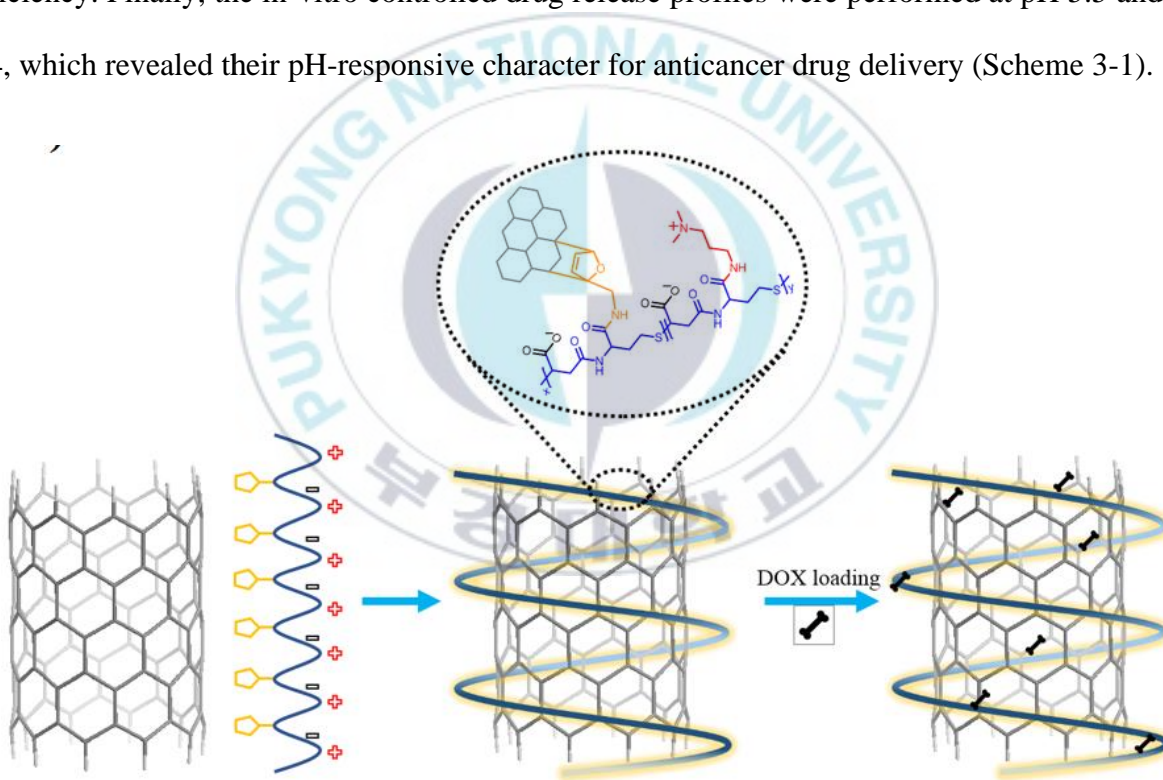
POLYAMPHOLYTES GRAFTED ONTO SINGLE-WALLED CARBON NANOTUBES BY DIELS-ALDER REACTION AND ITS APPLICATION IN DRUG DELIVERY

3.1 Introduction

Nanosized vehicles of attractive properties, such as metallic nanoparticles, polymeric micelles, and liposomes have been investigated to protect active pharmaceutical ingredients for drug delivery. Among these drug delivery systems, nanocarriers based on carbon nanotube materials and in particular single-walled carbon nanotubes (SWCNTs) have attracted much extensive attention as a potential candidate due to their great opportunities to use in biomedical applications such as bioimaging, biosensor and drug delivery [1-6]. Many studies have shown that CNTs had incomparable properties like biocompatibility, stability and diversity. Based on the diverse structure of CNTs (armchair, zigzag, and chiral configuration), they are conveniently modified with functional polymers and are applied as vehicles for biomedical applications. In addition, the drug loading capacity can be improved by the drug interactions with the internal hollow space (diameter varies between 0.4-3 nm) or external modified surface of SWCNTs [7,8]. However, the biggest limitation of SWCNTs is their water-insolubility, therefore, the outer surface of SWCNTs needs to be modified via chemical binding (covalent, non-covalent or ionic) [9,10,11]. Many functional polymers such as poly(ethylene glycol) and natural polymers such as polycarbohydrates have been used to modify the surface of SWCNTs [12,13,14]. Among various modification methods for SWCNTs the Diels Alder (DA) reaction showed many advantages such as simplicity,

non-catalysis and sympathetic solvents [15,16]. In general, this is a single-step cycloaddition reaction where SWCNTs play as dienophiles, which could provide a facile route for the synthesis of chemically grafted nanomaterials.

In this chapter, the resulting polymers were grafted onto the external surface of SWCNTs under ultrasonication in water to produce PMT/SWCNTs (Scheme 1). The polymer grafting greatly improved the dispersibility of SWCNTs in water and decrease their toxicity. Different ratios of furfuryl amine on the polyampholyte polymers were used to investigate the DOX loading efficiency. Finally, the in-vitro controlled drug release profiles were performed at pH 5.5 and pH 7.4, which revealed their pH-responsive character for anticancer drug delivery (Scheme 3-1).



Scheme 3-1. The preparation of polyampholytes grafted SWCNT for DOX loading.

3.2 Experimental section

3.2.1 Materials

Raw SWCNTs (product number ASA-100F, diameter 1-1.2 nm, length 5-20 μm) were purchased from Hanwha Nanotech (Korea) and then purified to remove metal impurities. DOX.HCl was kindly provided from Boryung Pharm. Co. (Korea). Human kidney cells (HEK293), and cervix cancer cells (HeLa) were obtained from ATCC (Manassas, VA, USA) and grown in minimum essential medium (MEM; Corning, Manassas, VA, USA) containing heat-inactivated fetal bovine serum (10%) and antibiotics (1%). Cells were grown and maintained under humidified condition with 5% CO_2 at 37 $^\circ\text{C}$. The cell viability assay was performed as per methodology reported previously [17].

3.2.2 Synthesis of SWCNTs/PMTs hybrids

A mixture of 0.2 g of PMT, 0.2 g of KOH and 100 mg of SWCNTs in 200 mL of deionized water was placed in an ultrasonication bath at 60 $^\circ\text{C}$ for 2 h. By using a 0.2 μm PTFE membrane, the unreacted polymers were removed by 200 mL of water. To investigate the drug loading capacity of hybrid materials, the PMT/SWCNTs was dispersed in 200 mL (0.01 M, pH 7.4) of PBS and adjusted up to pH 8.0.

3.2.3 Characterization

Optizen POP was used to record the UV-Vis spectra. Thermogravimetric analysis (TGA) was conducted by using A Perkin Elmer Pyris 1 analyzer (USA) within the temperature range of 50-700 $^\circ\text{C}$ at a heating rate of 10 $^\circ\text{C min}^{-1}$ under air flow. The dispersed hybrids on carbon coated copper grid was characterized using a transmission electron microscopy (TEM) JEOL JEM-2010. Raman spectra were obtained by measuring the solution after reaction directly using Raman system (PeakSeeker PRO-785), with a 785 nm diode laser.

3.2.4 In-vitro drug loading and release study

For the investigation of DOX loading and drug release profile, PMT/SWCNTs and DOX were separately dispersed in PBS 0.01 M solutions so that their concentrations were 0.1 mg/mL and 1 mg/mL, respectively. These solutions were mixed together by ratio 1:2 wt./wt. of PMT/SWCNTs: DOX, adjusted to pH 8.0 and stirred at room temperature in the dark for 24 h. By using a 0.2 µm PTFE membrane, the DOX-loaded complexes were filtered out and re-dispersed in 40 mL of PBS (0.01 M, pH 7.4). The filtrate solution was measured by UV-Vis absorbance at 490 nm to calculate the quantity of the amount of free DOX. The below formulas were applied to determine the drug loading efficiency (DLE) and drug loading capacity (DLC):

$$\text{DLE \%} = \frac{\text{weight of loaded drug in SWCNTs}}{\text{weight of drug in feed}} \times 100$$
$$\text{DLC \%} = \frac{\text{weight of loaded drug in SWCNTs}}{\text{total weight of drug-loaded SWCNTs}} \times 100$$

PBS solutions at pH 5.5 and pH 7.4 were used to mimic the lysosomal and physiological pH at 37 °C for the investigation of in vitro drug release profiles of DOX/SWCNT complexes. 3 mL of the DOX-loaded SWCNTs solution was put in a dialysis bag (MWCO = 13 kDa) and sequentially stirred in 20mL of PBS solution (pH 5.5 and pH 7.4) at 37 °C. Afterwards, 3 mL of the solution was taken out in time-intervals (2, 4, 6, 12, 24, 48 and 72 h) to quantify the concentration of released DOX by measuring the UV-Vis absorbance at 490 nm. 3 mL of the buffer solution was added at the same condition for maintaining the volume of release media.

3.2.5 Cell viability

Cytotoxicity of PMT/SWCNTs was determined on HEK293 cells, and PMT/SWCNT/DOX and only DOX were tested on HeLa cells. Both cells, 1×10^4 cells were added on each well of 96-well plates and incubated for 24 h, after that treated with different concentrations of PMT/SWCNT (20, 40, 60, 80, and 100 $\mu\text{g/ml}$), PMT/SWCNT/DOX (0.1, 0.5, 1, 5, 10, and 15 $\mu\text{g/ml}$), and only DOX (0.1, 0.5, 1, 5, 10, and 15 $\mu\text{g/ml}$) for 24 h. After incubation, fresh media were replaced and 10 μl of cell viability solution WST-1[®] (Daeil Lab Service, Gyeonggi, Korea) added to each well and incubated for 3 h. Cell viability were measured using Varioskan LUX microplate reader (Thermo Fisher Scientific Inc., USA) by measuring the absorbance at 460 nm.

3.3 Results and discussion

3.3.1 Surface functionalization of SWCNT

For the evaluation of the grafting process, PMTs and PMT3/SWCNT hybrids were characterized by means of FT-IR and Raman spectroscopy, as shown in **Figure 3-1**. The FT-IR spectrum of PMT3 displays characteristic bands of tertiary amine, secondary amine, carbonyl and furfuryl groups at 2650, 1603, 1700 and 1370 cm^{-1} , and at 600 and 750 cm^{-1} , respectively (**Figure 3-1c**). As compared with SWCNTs, the spectrum of PMT3/SWCNT hybrids clearly exhibits new characteristic bands corresponding to the vibration of functional groups in the PMT chain, indicating the successful functionalization of SWCNTs with polyampholytic PMTs.

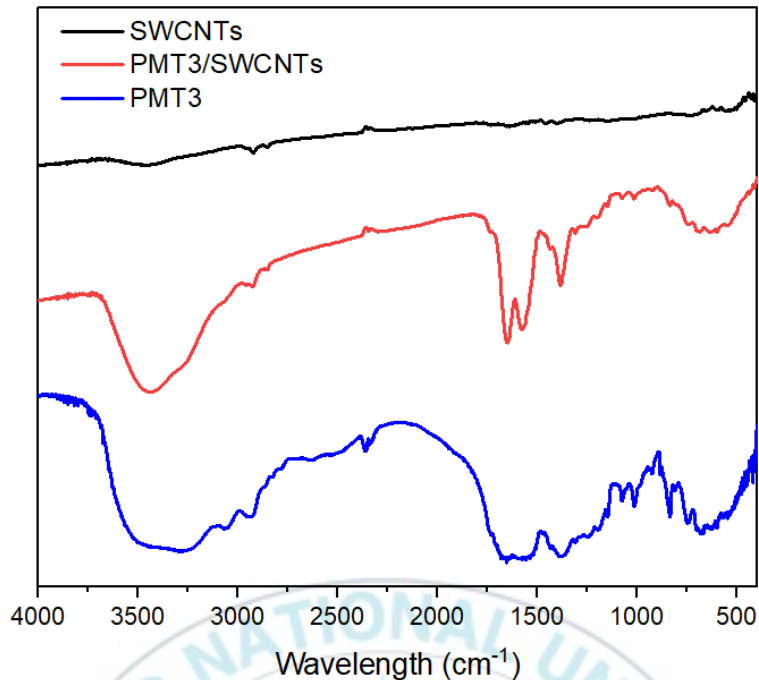


Figure 3-1. FT-IR spectra PMT3 and SWCNTs before and after grafting with PMT3

Raman spectroscopy was applied to evaluate the D-band with the shift around 1350 cm^{-1} which is attributed to the obstruction in the curved graphene layers/tube ends and the G-band with the shift around 1576 cm^{-1} which corresponds to the movement in the opposite direction of two neighboring carbon atoms in a graphene sheet. The intensity ratio I_D/I_G is known to depend on the structural properties of the CNTs due to the modification of sp^2 (C-C) to sp^3 (C-C) bonds in the structure of CNTs. An increase in I_D/I_G corresponds to a higher proportion of sp^3 carbons, which is usually attributed to the presence of more structural defects. The values of I_D/I_G ratio of PMT/CNTs increased from 0.8 to 1.06 corresponding to the increasing of furfuryl amine groups in PMT1, PMT2 and PMT3 (**Figure 3-2**), which were higher than the value of pristine SWCNTs (0.48) (**Figure 3-2a**). The result reveals that the increase of defects in the characteristics of SWCNTs was induced by the DA reaction.

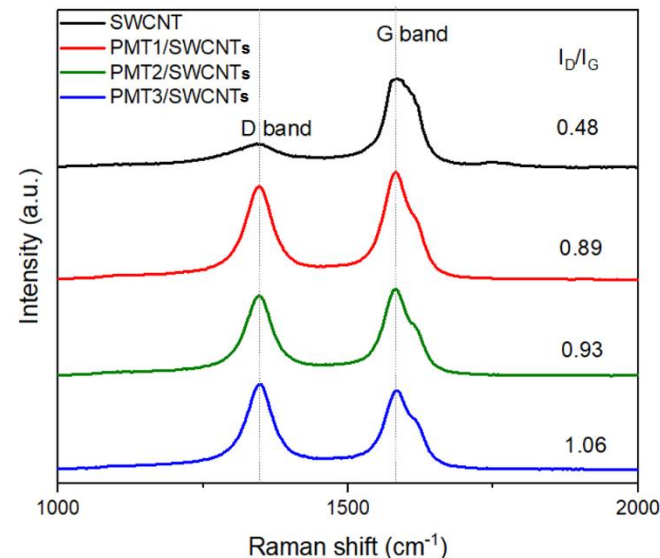


Figure 3-2. Raman spectra of SWCNTs (a) before modification, modified with (b) PMT1, (c) PMT2 and (d) PMT3.

TGA study was carried out to investigate the thermal stability of the PMT/SWCNT hybrids. The amount of PMTs grafted on SWCNTs was also determined by means of TGA. As can be seen in **Figure 3-3a**, PMTs show two-stage degradation. The first degradation occurs around at 170 °C and the second one happens at 240 °C. It is difficult to identify the degradation rate in the TGA of the PMT/SWCNT hybrid. The weight loss peak around 150 ~ 260 °C is possibly attributed to the amount of PMTs grafted on the SWCNT surface. The TGA analysis shows that the weight losses of the PMT/SWCNTs hybrid produced from PMT1 and PMT2 are 11.04 % and 11.93 %, respectively. While, 13.56 % of grafting is observed for PMT3. The grafting ratios of PMT/SWCNTs are summarized in **Table 2-1**. These results indicate that the increase of furfuryl amine groups in the PMT polymers leads to the increase in the grafting density of the hybrid.

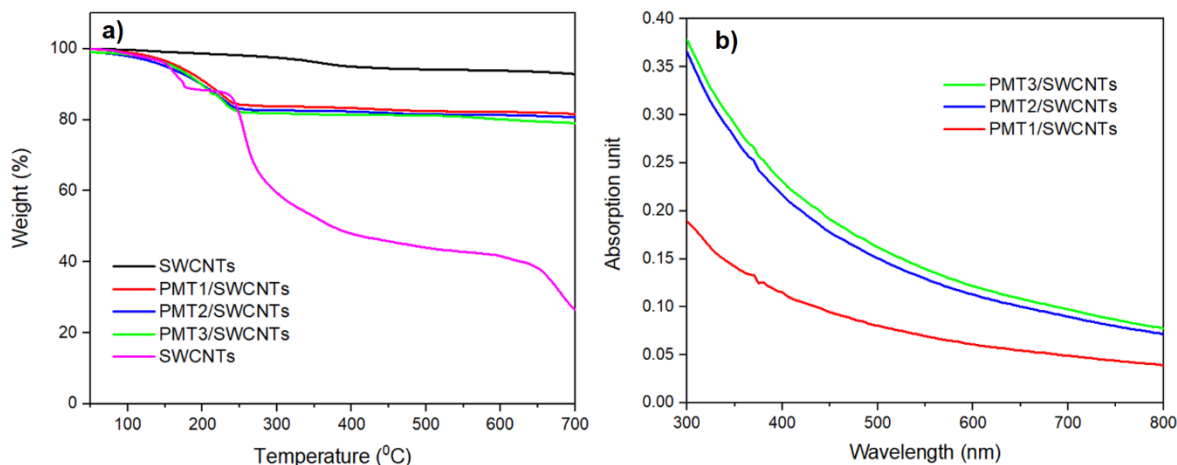


Figure 3-3. a) TGA curves of pristine SWCNT, PMTs, and PMTs/SWCNT; b) UV-Vis spectra of aqueous dispersants of PMTs/SWCNT.

UV-Vis spectroscopy was used as a common method to evaluate the degree of dispersion of SWCNTs in a solvent. It is well known that SWCNT bundles are not stimulated in the wavelength range between 300 and 800 nm whereas individual SWCNT can absorb light in the UV-Vis region. The quality of suspension depends on the individualization of SWCNTs in an aqueous solution, which affects the intensity of the absorption spectrum. The supernatant of PMT/SWCNTs suspensions was collected after centrifugation. **Figure 3-3b** shows the spectroscopy of the supernatant of PMT/SWCNTs suspensions. It can be observed that the absorbance intensity increases with increasing furfuryl amine pendants in the PMT formulation, while pristine SWCNTs yield a very clear supernatant, illustrating the successful modification of SWCNTs by the DA click reaction.

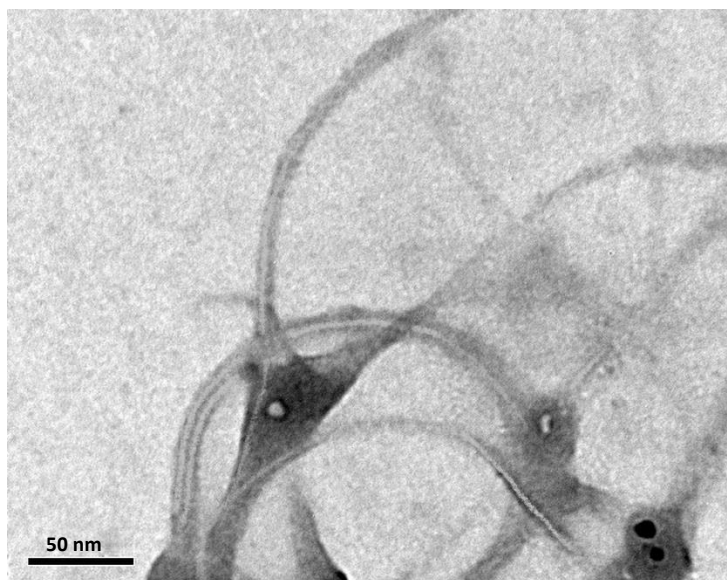


Figure 3-4. TEM images of PMT/SWCNTs after the surface modification by DA reaction.

TEM analysis was performed for the samples after modification to investigate the effects of the grafting process on the surface of SWCNTs. As can be seen in **Figure 3-4**, the TEM image only shows a simple structure and property of SWCNTs with the thickness of 2 ± 0.3 nm. After the DA reaction, the surface of initial CNTs are covered by PMT polymers. The polymer layer thickness was calculated around 4 nm. The results also indicate the successful grafting of the functional polymer onto the surface of SWCNTs.

3.3.2 In-vitro drug loading and release study

Dispersant polymer	Feed ratio (w/w)	DLC	DLE
	m _{DOX} /m _{PMT/SWCNT}	(wt.%)	(wt.%)
PMT1/SWCNT	200	71.3	143
PMT2/SWCNT	200	78.8	149
PMT3/SWCNT	200	74.3	158

Table 3-1. DOX encapsulation of PMT/SWCNTs

For the investigation of pharmaceutical ingredient loading onto the modified SWCNT surface, Doxorubicin (DOX), an anticancer drug was chosen as a model drug. DOX can be adsorbed on the outer surface of SWCNTs by π - π stacking interactions as well as encapsulated in the inner space of SWCNT [18,19].

The number of furfuryl amine moieties was varied while the feed ratio between DOX and PMT/SWCNTs was kept at 200% in order to investigate whether DOX was effectively loaded on PMT/SWCNT hybrids. The DLC and DLE of the drug loaded SWCNT hybrids are summarized in **Table 3-1**. The values of DLE increased from 143 to 158 corresponding to the increasing ratio of furfuryl amine pendants in PMT/SWCNTs. On the other hand, the DLEs were not consistent among them, which were 71.3 % in PMT1, 78.8 % in PMT2, and 74.3 % in PMT3. The result could be explained by the fact that the limit of loading capacity was reached when polymer grafting density increased from PMT1 (71.3 %) to PMT2 (78.8 %), and the drug was pushed out during the loading process to result in lower DLC at PMT3 (74.3 %). In the drug delivery application of CNTs, SWCNTs were proven to have more efficient drug-loading capacity than other kinds of CNTs owing to the ultra-high surface area. In this study, the DLC of PMT/SWCNTs was calculated to be more than 150% when compared with feed ratio (200 %), which confirmed the great loading capacity of SWCNT based hybrid materials. PMT1/SWCNTs and PMT2/SWCNTs were selected for further experiments to evaluate the drug release profiles under the effects of charge compensation.

The DOX release profiles of SWCNT hybrids were performed in phosphate buffer saline (pH 7.4) and acetate buffer (pH 5.5) solutions at 37 °C to identify the pH responsive release ability of DOX loaded PMT/SWCNTs (**Figure 3-5**). The in vitro profiles showed that 16.3 % and 27.6 % of DOX

were released from PMT1/SWCNT and PMT3/SWCNT at pH 7.4 after 72 h. There was a significant release of DOX was observed at pH 5.5 after 72 h which up to 71.2 % and 77.9 % from PMT1/SWCNT and PMT3/SWCNT. The triggered release profile could be based on the phenomenon that the diffusion of DOX was speeded up at the low pH because of the increase in DOX solubility and the increase in hydrophobic effects by the protonation of carboxylic groups [20,21]. These results clearly represent the acid responsive behavior of DOX-PMT/SWCNTs for a burst release of DOX, which suggests that these materials have a potential application in the release of pharmaceutical ingredients at acidic lysosomal environment.

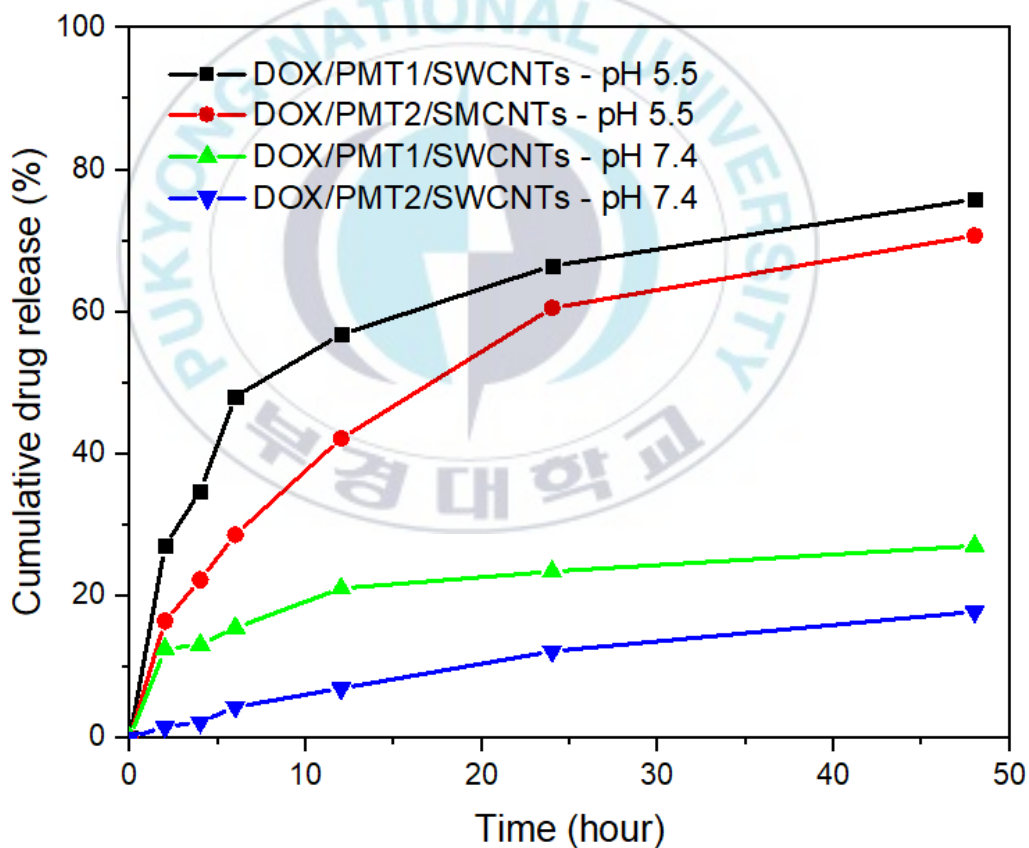


Figure 3-5. pH responsive DOX release profile of DOX/PMT1/SWCNTs and DOX/PMT2/SWCNTs.

3.3.3 Cytotoxicity of blank PMT1/SWCNTs and DOX/PMT1/SWCNTs

We evaluated the cytotoxicity of PMT1/SWCNTs, DOX/PMT1/SWCNTs and only DOX on normal and cancerous cell lines using the colorimetric method. WST reagent assay is commonly applied for cytotoxicity determination. **Figure 3-6a** indicates that PMT1/SWCNTs had no growth inhibitory effect on HEK293 cells. On the other hand, the DOX/PMT1/SWCNTs and only DOX had concentration dependent cytotoxic effects on HeLa cells (**Figure 3-6b**). Only DOX showed more cytotoxicity on HeLa cells compared to DOX/PMT1/SWCNTs possibly due to the higher availability of DOX to interact with cell constituents and inhibit cells growth. DOX/PMT1/SWCNTs showed increasing cytotoxicity from lower to higher concentration on HeLa cells. The cells viability was observed 99.47%, 92.02%, 80.08%, 31.04%, 23.19%, and 20.87% with the concentration 0.1, 0.5, 1, 5, 10, and 15 $\mu\text{g/ml}$ of DOX/PMT1/SWCNTs, respectively. This significant cytotoxicity can be attributed to the specific dependence on the controlled release of DOX from DOX/PMT1/SWCNTs. The drug loaded onto the hybrids have less cytotoxicity effect compared to free DOX, which is based on the fact that drug release requires time and depends on surrounding pH conditions [22]. Consequently, PMT/SWCNT/DOX could be attractive in anticancer therapy with combined treatment effect of DOX and controlled release at pH environment [8].

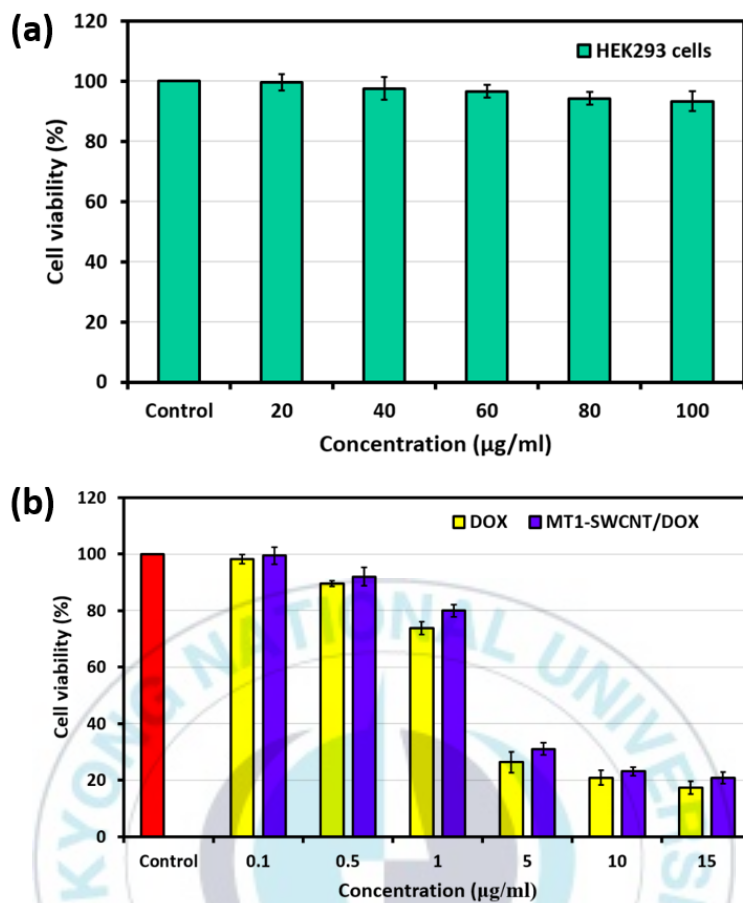


Figure 3-6. Cells viability determined by WST-1[®] method a) with HEK293 cells after 24 h incubation with different concentrations of PMT/SWCNTs and b) with HeLa cells after 24 h incubation with different concentrations of PMT/SWCNT/DOX and only DOX. Error bars above the bars indicates \pm standard deviation (n=3).

3.4 Conclusions

A smart functionalization strategy of SWCNTs was achieved by a green process using water. The alternating polyampholytes were successfully synthesized and functionalized via thiol-ene chemistry in aqueous medium under ambient conditions. The SWCNT hybrids were prepared through the Diels-Alder reaction under ultrasonication, as evidenced by ¹H NMR, FT-IR, TGA

and UV-vis. The PMT/SWCNTs demonstrated a high loading capacity of DOX up to 150 %. Besides, these hybrids showed pH-responsive drug release with a burst release at pH 5.5 while the release behavior was remained stable at pH 7.4. The cell viability and cytotoxicity toward normal cells HEK293 and cancer cells HeLa indicated the high efficiency in tumor treatment. The combination of “green” thiol-ene and Diels-Alder chemistry in the preparation of polyampholytes grafted SWCNTs promises not only a potential vehicle for drug delivery applications but also reduction of organic solvents in pharmaceutical industry.

3.5 References

1. Bianco, A.; Kostarelos, K.; Prato, M., *Curr. Opin. Chem. Biol.* **2005**, 9 (6), 674-679.
2. Bianco, A.; Kostarelos, K.; Partidos, C. D.; Prato, M., *Chem. Commun.* **2005**, (5), 571-577.
3. Prato, M.; Kostarelos, K.; Bianco, A., *Acc. Chem. Res.* **2007**, 41 (1), 60-68.
4. He, H.; Pham-Huy, L. A.; Dramou, P.; Xiao, D.; Zuo, P.; Pham-Huy, C., *BioMed research international* **2013**, 2013.
5. Meng, L.; Zhang, X.; Lu, Q.; Fei, Z.; Dyson, P. J., *Biomaterials* **2012**, 33 (6), 1689-1698.
6. Liu, Z.; Chen, K.; Davis, C.; Sherlock, S.; Cao, Q.; Chen, X.; Dai, H., *Cancer Res.* **2008**, 68 (16), 6652-6660.
7. Dillon, A. C.; Jones, K.; Bekkedahl, T.; Kiang, C.; Bethune, D.; Heben, M., *Nature* **1997**, 386 (6623), 377.
8. Gu, Y.-J.; Cheng, J.; Jin, J.; Cheng, S. H.; Wong, W.-T., *International journal of nanomedicine* **2011**, 6, 2889.
9. Prakash, S.; Kulamarva, A. G., *Recent patents on drug delivery & formulation* **2007**, 1 (3), 214-221.

10. Merum, S.; Veluru, J. B.; Seeram, R., *Materials Science and Engineering: B* **2017**, 223, 43-63.
11. Huang, Y. Y.; Terentjev, E. M., *Polymers* **2012**, 4 (1), 275-295.
12. Lay, C. L.; Liu, J.; Liu, Y., *Expert Rev. Med. Devices* **2011**, 8 (5), 561-566.
13. Gorityala, B. K.; Ma, J.; Wang, X.; Chen, P.; Liu, X.-W., *Chem. Soc. Rev.* **2010**, 39 (8), 2925-2934.
14. Chen, Y.; Star, A.; Vidal, S., *Chem. Soc. Rev.* **2013**, 42 (11), 4532-4542.
15. Le, C. M.; Cao, X. T.; Lim, K. T., *Ultrason. Sonochem.* **2017**, 39, 321-329.
16. Pramanik, N. B.; Singha, N. K., *RSC Advances* **2015**, 5 (114), 94321-94327.
17. Salma, S. A.; Patil, M. P.; Kim, D. W.; Le, C. M. Q.; Ahn, B.-H.; Kim, G.-D.; Lim, K. T., *Polymer Chemistry* **2018**, 9 (39), 4813-4823.
18. Madani, S. Y.; Naderi, N.; Dissanayake, O.; Tan, A.; Seifalian, A. M., *International journal of nanomedicine* **2011**, 6, 2963.
19. Jin, S.; Wan, J.; Meng, L.; Huang, X.; Guo, J.; Liu, L.; Wang, C., *ACS applied materials & interfaces* **2015**, 7 (35), 19843-19852.
20. Le, C.; Cao, X.; Tu, T.; Gal, Y.; Lim, K., *eXPRESS Polymer Letters* **2018**, 12 (8), 688-698.
21. Cuggino, J. C.; Molina, M.; Wedepohl, S.; Igarzabal, C. I. A.; Calderón, M.; Gugliotta, L. M., *Eur. Polym. J.* **2016**, 78, 14-24.
22. Yan, C.; Chen, C.; Hou, L.; Zhang, H.; Che, Y.; Qi, Y.; Zhang, X.; Cheng, J.; Zhang, Z., *J. Drug Targeting* **2017**, 25 (2), 163-171.

ACKNOWLEDGEMENT

First of all, I am heartily thankful to my supervisor, Prof. Kwon Taek Lim, not only for giving me an opportunity to join in this academic environment, but also for his valuable guidance, encouragement and inspiration in my academic career.

I am very grateful to the thesis evaluation committee, Prof. Yeon Tae Jeong and Prof. Jong Tea Kim for their support, constructive criticism and valuable input. Moreover, I would like to take this opportunity to thank all professors in the Display Engineering Department, Pukyong National University for their support and encouragement.

For the financial support, I would like to express my sincere gratitude to Pukyong National University and BK21 Plus program for providing me a scholarship for the entire period of my study in Korea.

I also thank my lab-mates and friends at Display Engineering Department for valuable friendship. Especially, I would like to express my appreciation to Dr. Maheshkumar Prakash Patil for helping to obtain the biological characterization.

Last but not least, there are no words to express my thanks and feelings to my parents for encouraging me to study abroad; and specially my beautiful girlfriend Ngan Pham, for her endless support and love without asking any rewards.